Carbon sequestration in an expanding lake system during the Toarcian Oceanic Anoxic Event

Weimu Xu[1]*, Micha Ruhl[1], Hugh C. Jenkyns[1], Stephen P. Hesselbo[2], James B. Riding[3], David Selby[4], B. David A. Naafs[5], Johan W.H. Weijers[6], Richard D. Pancost[5], Erik W. Tegelaar[6], Erdem F. Idiz[1]

[1]Department of Earth Sciences, University of Oxford, Oxford OX1 3AN, UK (*Correspondence: weimu.xu@earth.ox.ac.uk)

[2]Camborne School of Mines and Environment and Sustainability Institute, University of Exeter, Penryn TR10 9FE, UK

[3]British Geological Survey, Keyworth, Nottingham NG12 5GG, UK

[4]Department of Earth Sciences, University of Durham, Durham DH1 3LE, UK

[5]Organic Geochemistry Unit, School of Chemistry and Cabot Institute, University of Bristol, Bristol BS8 1TS, UK

[6]Shell Global Solutions International B.V., Rijswijk 2288 GS, The Netherlands

The Early Jurassic Toarcian Oceanic Anoxic Event (~183 Ma) was marked by marine anoxia–euxinia and globally significant organic-matter burial, accompanied by a major global carbon-cycle perturbation probably linked to Karoo-Ferrar volcanism. Although the Toarcian Oceanic Anoxic Event is well studied in the marine realm, accompanying climatic and environmental change on the continents is poorly understood. Here, utilizing radiometric, palynological and geochemical data from lacustrine black shales, we demonstrate that a major lake system developed contemporaneously with the Toarcian Oceanic Anoxic Event in the Sichuan Basin, China, likely due to enhanced hydrological cycling under elevated atmospheric pCO_2. Coeval accelerated organic-carbon burial in both marine and lacustrine basins suggests nutrient delivery as the prime cause for global carbon-cycle recovery during the Toarcian Oceanic Anoxic Event. Increased lacustrine organic productivity from elevated fluvial nutrient supply resulted in the burial of ~460 Gt of organic carbon in the Sichuan Basin alone,

creating an important negative feedback in the global exogenic carbon cycle, which significantly shortened the global $\delta^{13}C$ recovery.

The early Toarcian Oceanic Anoxic Event (T-OAE at ~183 Ma) is recognized as one of the most intense and geographically extensive events of oceanic redox change and accompanying organic-carbon burial in the Mesozoic Era[1,2]. The T-OAE is marked by major changes in global geochemical cycles, with an apparently rapid negative shift of as much as ~7‰ in bulk marine and terrestrial organic-carbon isotope records and a typically smaller (3–6‰) negative excursion in carbonate archives and specific organic compounds[3-10]. The observed early Toarcian perturbation to the exogenic carbon cycle has been linked to volcanism of the Karoo-Ferrar large igneous province (LIP) and associated release of volcanogenic CO_2, thermogenic methane (CH_4) from sill intrusion into Gondwanan coals, and biogenic methane from dissociation of sub-seafloor clathrates[3,6,11-13]. Early Toarcian elevated atmospheric pCO_2 likely induced climatic and environmental change[5,12,14-16] by accelerating the global hydrological cycle and increasing silicate weathering, thereby increasing delivery of riverine nutrients to the oceans and potentially also to large inland lakes[17]. In the marine realm, the consequential increase in primary productivity and carbon flux to the sea floor is credited with enhancing the burial of planktonic material in relatively deep continental-margin sites, whereas in shallower water semi-restricted marine basins, chemical and physical water-column stratification likely aided the burial of organic matter[17]. Particularly in northern Europe, the evidence points to regional to global development of anoxic/euxinic (sulphide-rich) bottom waters that strongly affected palaeoceanographic conditions and marine ecosystems[15,17,18]. Globally significant burial of ^{13}C-depleted photosynthetically derived organic matter commonly produced

55 an overarching positive carbon-isotope excursion (CIE) interrupted by the
56 characteristic abrupt negative shift that invariably characterizes the T-OAE (early
57 Toarcian *tenuicostatum–falciferum* ammonite biozones)[1,2,18].

58 Marine records of the T-OAE, based on the presence of apparently coeval
59 organic-rich shales, have now been identified from many outcrops in both the
60 northern and southern hemispheres[2,5], but climatic and environmental change on the
61 continents is still poorly understood. Intriguingly, however, sedimentary archives
62 from continental interiors in China (e.g. the Tarim, Ordos and Sichuan Basins) are
63 consistently marked by the occurrence of organic-rich black shales that are latest
64 Early Jurassic in age[19-21]. This stratigraphic evidence suggests that major inland lakes
65 potentially formed or expanded contemporaneously with the T-OAE. Here, we (1)
66 determine the precise age of the upper Lower Jurassic lacustrine organic-rich black
67 shales in the Sichuan Basin; (2) determine their depositional context; and (3) explore
68 the possible relevance of major lake formation as an additional sink for carbon in the
69 context of the major disturbance in the early Toarcian exogenic carbon cycle.

70

71 AGE AND STRATIGRAPHY

72 The present-day topographic Sichuan Basin covers a total area of ~230,000 km^2 (ref.
73 22), almost three times the size of Lake Superior (82,100 km^2), the most extensive
74 modern freshwater lake in the world. The Early Jurassic Sichuan Basin (and the
75 palaeo-Sichuan lake system) is thought to have been even larger than its present-day
76 confines[23] (Fig. 1). Two cores, named A and B, (Fig. 1) were taken from the more
77 proximal, northwestern part of the Sichuan Basin, each penetrating the entire
78 Da'anzhai Member, which is ~50–70 m in thickness here. The Da'anzhai Member in
79 both successions exhibits alternating beds of fossiliferous carbonate and a spectrum of

mudrocks from clay-rich marl to laminated black shale (Fig. 2). Diverse freshwater bivalves, ostracods, gastropods and conchostracans in the fossiliferous carbonate beds and mudstone beds confirm these sediments to be lacustrine deposits[24]. The freshwater ostracod faunal assemblages, which include *Darwinula* spp. and *Metacypris unibulla,* suggest a late Early Jurassic age[25].

Here, palynostratigraphy, Re-Os chronology and chemostratigraphy are utilized to constrain further the depositional age of the Da'anzhai Member (see Methodology-section [2] for more detailed discussion). Re-Os radio-isotopic dating of 16 samples from two combined intervals of the Da'anzhai lacustrine black shale (Core A) provides a well-constrained single isochron of 180±3.2 Ma (Fig. 3; Supplementary Information Fig. S1), constraining the Da'anzhai Member to be of Toarcian age[26]. The palynomorph assemblages obtained from the studied cores closely resemble floras from lower Toarcian marine successions in northern Europe and Australia, further suggesting a similar depositional age for the lacustrine Da'anzhai Member (see Methodology-section [2]). The observed parallel signature in $\delta^{13}C_{TOC}$ (Cores A and B) and $\delta^{13}C_{n\text{-alkane}}$ (Core A) in the main phase of the Da'anzhai Member (above 2698 m) (Figs 2 and 3) likely reflects a true perturbation of the global exogenic carbon cycle (see Methodology-section). It is similar in shape and magnitude to what is characteristically observed in early Toarcian marine calcite and compound-specific marine and terrestrial organic- matter records from Europe and elsewhere spanning the T-OAE[4,8–10] (Fig. 3).

The combined macro- and microfossil biostratigraphy, palynostratigraphy, Re-Os chronology and chemostratigraphy uniquely constrain the formation of the Da'anzhai Member to be time-equivalent with the T-OAE.

DEPOSITIONAL ENVIRONMENT OF THE DA'ANZHAI MEMBER

Terrestrial (fluvial/deltaic and soil) deposits of the Ma'anshan Member in the mid-Early Jurassic Sichuan Basin pass up-section into the lacustrine facies of the Da'anzhai Member. Chemostratigraphic correlation between the more distal Core A and the more proximal Core B, based on elevated total organic carbon (TOC) and HI and the observed $\delta^{13}C_{TOC}$ negative CIE, suggests a diachronous base of the Da'anzhai Member, as defined by the presence of characteristic lacustrine facies lying stratigraphically above palaeosols (Fig. 2). The lower half of the Da'anzhai Member in Core A is marked by abundant fossiliferous limestone, primarily consisting of bivalve and ostracod shell fragments, alternating with more clay-rich sediments. This interval is also marked by generally low TOC (~1%) and HI values (~150 mg C/g TOC), suggesting a near-shore depositional environment with low aquatic organic matter productivity and/or preservation. The abrupt transition from palaeosol to fossiliferous limestone at ~2714.85 m, followed by the transition to laminated organic-rich black shale at ~2693.40 m in the more distal Core A, and the coeval transition from palaeosol to laminated organic-rich black shale at ~3156.34 m in Core B (Fig. 2), suggests the rapid expansion and deepening of the lake, with decreased macrofossil carbonate supply (Fig. 4). Macrofossils in the regularly occurring limestone beds show variable orientation and degrees of fragmentation and, depending on the stratigraphic horizon, are in life position, or were subjected to local transport and re-deposition. The interbedded marls and black shales are interpreted as representing quieter water sedimentation and/or sedimentation inimical to benthic life.

The fossil assemblages from both cores signify a predominantly non-marine depositional environment, with the occurrence of the freshwater bivalve genus *Margaritifera*[24], lacustrine ostrocods, and the freshwater/brackish alga *Botryococcus*

(Supplementary Information). However, some intervals in Core A (2684.49 m to 2695.80 m and 2702.49 m to 2710.73 m) contain *in situ* marine palynomorphs such as the acritarch *Veryhachium collectum* and the prasinophyte *Halosphaeropsis liassica* (Fig. 2, Supplementary Information). These occurrences suggest marine incursions into the basin. Significantly, the oldest sediments of the lacustrine Da'anzhai Member studied in Core A are devoid of acritarchs (Fig. 2; Supplementary Information), indicating that the lake had already developed before any potential marine incursion took place. Furthermore, the relative abundance of acritarchs in the samples studied shows no positive correlation with TOC or (pyritic) sulphur abundance (Figs 2 and 3), indicating that deposition of the most organic-rich sediments and the supply of sulphate was unrelated to a potential marine connection. Sedimentary facies in Europe and elsewhere indicate that the early Toarcian witnessed a significant marine transgression, culminating in the *falciferum* ammonite biozone[27,28]. Although the Early Jurassic Sichuan Basin was surrounded by compressional mountain ranges in the north, east and west, the palaeo-Sichuan lake system likely formed close to sea level and the basin could, therefore, have been temporarily connected to the ocean to the south (Fig. 1 and references herein, Fig. 4). Overall, however, the abundance of freshwater fossils and palynomorphs, combined with a highly elevated radiogenic initial $^{187}Os/^{188}Os$ composition of ~1.29, significantly higher than Early Jurassic Toarcian open marine $Os_{initial}$ values of 0.4−0.8 recorded from Europe[29] (Supplementary Information), points to a dominantly lacustrine environment during the deposition of the Da'anzhai Member. This interpretation is further supported by the presence of tetracyclic polyprenoids (TPP) (typically sourced from freshwater algae; Supplementary Information Fig. S5), the near absence of C_{30} steranes (typically

154 sourced from marine algae; Supplementary Information Fig. S6) and high hopane
155 over sterane biomarker ratios throughout Core A[30,31] (Supplementary Information).

156 Previous study on a section from Bornholm, Denmark suggested a sharp
157 increase of atmospheric pCO_2 reconstructed from terrestrial leaf stomatal density at
158 the onset of the negative CIE[12]. The increased occurrence of *Classopollis* in tetrads
159 (relative to single specimens; Fig. 2) observed during the negative CIE interval
160 suggests stressed environmental conditions on land during the T-OAE, likely in
161 response to enhanced atmospheric pCO_2 and greenhouse-gas-induced climatic
162 warming[12,14,18,32,33].

163 The Toarcian mid-palaeolatitude setting and geomorphology of the palaeo-
164 Sichuan Basin, with surrounding high mountain ranges[21], may have made the basin
165 susceptible to an enhanced monsoonal system and increased hydrological cycle with
166 high amounts of run-off, particularly when warm shallow transgressive seas
167 approached (Fig. 4) (cf. the modern South Asian monsoon[34]). The formation or strong
168 expansion of the palaeo-lake system in the early Toarcian Sichuan Basin, with the
169 deposition of the Da'anzhai Member lacustrine black shales with elevated TOC (of up
170 to ~3.3%) and HI (of up to 450 mg HC/g TOC) levels, suggests increased aquatic
171 primary productivity due to increased continental weathering and accelerated riverine
172 nutrient supply. Significantly, based on all the stratigraphic data herein (Fig. 3), the
173 level of maximum TOC enrichment in the Da'anzhai Member developed coevally
174 with the most organic-rich black shale in marine sections from Yorkshire, UK (Fig.
175 3), consistent with a fundamental global climatic control on the introduction of
176 nutrients into aquatic environments, even though the quantity and type of organic
177 matter deposited and preserved may have been different.

Elevated sulphur concentrations in the most organic-rich sections of laminated black shale of the Da'anzhai Member in Core A (Fig. 3; Supplementary Information), coincide with the occurrence of small (<5 μm diameter) and also larger pyrite framboids (Supplementary Information Fig. S11). The source of sulphur is, however, as yet uncertain, but lake sulphate could have originated from the weathering of the Lower–Middle Triassic evaporites in the hinterland[22]. Although the larger pyrite framboids could have formed diagenetically in sulphide-rich sedimentary pore-waters, the smaller framboids (<5 μm) likely formed by sulphate reduction in the water column, as typically happens under euxinic conditions[35]. The stratigraphic intervals with high (pyritic) sulphur concentrations coincide with levels of elevated sedimentary molybdenum enrichment (with Mo >20 ppm; Fig. 3). In oxic conditions, Mo exists as soluble molybdate (MoO_4^{2-}) that adsorbs onto Mn-oxides and only slowly precipitates. In sulphidic (euxinic) waters, however, molybdate dissociates into thiomolybdate anions, which are rapidly reduced to highly reactive Mo(IV)-sulphides that precipitate out of solution, leading to sedimentary Mo enrichment[36]. Furthermore, water-column stratification, which is a likely prerequisite for sustained euxinia, is also supported by elevated levels of gammacerane in the black-shale interval of Core A (Fig. 2; Supplementary Information). Gammacerane is a biomarker derived from tetrahymanol that forms in abundance under conditions of high bacterial productivity within stratified water columns, commonly in lakes or isolated marine basins[37]. The combined geochemical and mineralogical data suggest the development of a physically or chemically stratified water column during laminated black-shale formation in the palaeo-Sichuan Lake, even in relatively proximal depositional settings.

LACUSTRINE CARBON BURIAL AND THE TOARCIAN CARBON CYCLE

The early Toarcian negative CIE has been widely attributed to the release of ^{13}C-depleted volcanogenic CO_2 and/or methane from either thermal metamorphism of Gondwanan coals or the dissociation of sub-sea-floor gas hydrates, also resulting in enhanced early Toarcian atmospheric pCO_2 levels[3,11,12,15]. The typical early Toarcian $\delta^{13}C$ pattern, with a stepped negative shift interrupting an overarching positive excursion, has been observed in marine and terrestrial organic matter and shallow-water platform and deep-water pelagic carbonates and manifestly affected the entire ocean–atmosphere system[3,5,6,8]. The overall positive shift is attributed to globally accelerated organic-carbon burial whereas the superimposed stepped negative shift suggests that the release of isotopically light carbon took place in pulses that have been attributed to astronomical forcing of the global carbon cycle[6]. Astronomical interpretation of periodic fluctuations in chemical and physical proxy records estimate the duration of the early Toarcian negative CIE at 300−900 kyr[6,38–40].

In the early Toarcian Sichuan Basin, the laminated black-shale interval in both cores is marked by elevated HI and TOC values (with HI up to 450 mg HC/g TOC and TOC up to 3.3% in the more distal Core A), likely reflecting increased algal primary productivity, in addition to a background supply of terrestrial organic matter, during the interval with the lowest carbon-isotope values of the negative CIE. This chemostratigraphic pattern is very similar to that developed in marine sections from northern Europe, where sedimentary TOC-levels can locally reach ~20%. Box-model studies for the early Toarcian carbon cycle suggest that the release of ~9000 Gt carbon from methane clathrates (with $\delta^{13}C$ of ~ -60‰) or ~25,000 Gt carbon as thermogenic methane (with $\delta^{13}C$ of ~ -35‰), is required to generate a negative $\delta^{13}C$ excursion compatible with the mean change in bulk carbonate of 4–6‰, and which

would have caused an increase in atmospheric pCO_2 of ~1000 ppm[7,8,15,41]. Excess atmospheric CO_2 is assumed to have been sequestered both by enhanced weathering of Ca-Mg silicates due to greenhouse warming, and by massive burial of organic carbon in marine dysoxic, anoxic and euxinic depositional environments[17]. These combined processes would have dictated the pattern of $\delta^{13}C$ recovery, but the total amount of ^{13}C-depleted carbon released may have been even larger than modelled because enhanced ^{12}C-enriched carbon burial would have acted as a mechanism to potentially increase ocean-atmosphere $\delta^{13}C$ during the onset of the T-OAE, even though the resultant summed effect was to move values in the opposite direction.

Sequestration of carbon in marine basins is generally considered to have been a major driver behind $\delta^{13}C$ recovery. The sheer size of the latest Early Jurassic continental basins, and the expansion of this major lake in response to early Toarcian environmental change provide, however, an additional, and significant, sink for carbon. The Da'anzhai Member lacustrine black shale formed over 70,000 km^2 in the palaeo-Sichuan Basin, with an average thickness of 60−120 m and 0.8−3.5% TOC; lacustrine marl and carbonate accumulated coevally over large parts of the remaining 160,000 km^2 of the basin[42]. Applying the average of these parameters, it is estimated that ~460 Gt of organic carbon and ~1200 Gt of inorganic carbon was extracted from the global ocean–atmosphere system and sequestered in the palaeo-Sichuan lake during deposition of the lower Toarcian Da'anzhai Member black shales alone (Supplementary Information). This figure is, however, a conservative estimate because original sedimentary TOC values may have been even higher considering the present-day maturity of the rock. Also, TOC values in the deepest, most central part of the basin may have been more elevated than in the more proximal cores studied herein. Enhanced continental inorganic-carbon burial would not affect the isotopic

253 composition of exogenic carbon reservoirs, but the burial of isotopically depleted
254 organic carbon would shift the carbon-isotope composition of the global exogenic
255 carbon cycle to more positive values. Assuming the (pulsed) release of 9,000 Gt of
256 carbon from methane clathrates (with a $\delta^{13}C$ of ~ -60‰) or 25,000 Gt as thermogenic
257 methane (with a $\delta^{13}C$ of ~ -35‰) to explain the observed step-wise negative shift in
258 $\delta^{13}C$ (-5‰; from 1‰ to -4‰) during the T-OAE[41], and assuming global carbon
259 sequestration largely by organic-matter burial (with a $\delta^{13}C$ of -25‰) to explain the
260 observed recovery in global $\delta^{13}C$, a simple mass-balance model indicates that early
261 Toarcian organic carbon burial in the black shale of the palaeo-Sichuan Basin alone
262 sequestered 1.3−2.2% of the total amount sequestered to recover from the $\delta^{13}C$
263 negative shift during the T-OAE negative CIE (Supplementary Information). The
264 present-day global lake surface area is about ~0.69% of the surface area of the global
265 ocean; lakes, however, account for ~10% of the global carbon drawdown and burial[43].
266 The palaeo-Sichuan lake alone covered over ~230,000 km^2, which is ~10% of the
267 present-day global lake surface, but it was responsible for, at least, 1.3–2.2% of the
268 global organic carbon burial flux. The generation of massive sinks of carbon in the
269 early Toarcian continental interiors by the formation and/or expansion of major lakes
270 and subsequent sequestration of carbon, in addition to marine carbon burial,
271 potentially significantly impacts the nature and duration of the observed exogenic
272 carbon-cycle perturbation. If the carbon sink of the Sichuan Basin black shale had not
273 formed, and with the assumption of constant climatic/environmental parameters
274 affecting the rate of carbon drawdown, the recovery from the $\delta^{13}C$ negative shift
275 would have required an additional ~4,000–20,000 yr of global marine carbon
276 drawdown (Supplementary Information). In addition, massive burial of inorganic
277 carbon in the Sichuan Basin, extracted from the ocean–atmosphere system, would

have significantly lowered atmospheric pCO_2, which likely further shortened the Early Toarcian climatic perturbation. Given that several other lacustrine basins, for example, the Tarim and Ordos Basins in northwestern and central northern China (Fig. 1) also appear to have developed in the late Early Jurassic with the deposition of organic-rich sediments[19,20], these figures are undoubtedly minima.

These results suggest an as-yet-unexplored, negative feedback in the global exogenic carbon cycle during oceanic anoxic events. Climatic warming induced by addition of greenhouse gases to the atmosphere, and an associated increase in hydrological cycling, allowed for the formation of major lake systems in continental settings, where enhanced fluvial nutrient supply with increased productivity and preservation could have lead to major carbon sequestration. Together with widespread burial of organic matter in the marine realm, the lacustrine carbon sink would have reduced atmospheric pCO_2, allowed rebound of the global $\delta^{13}C$ signal, and cooled global climate through an inverse greenhouse effect[18].

References

1. Jenkyns, H. C. The early Toarcian and Cenomanian-Turonian anoxic events in Europe: comparisons and contrasts. *Geol. Rundsch.* **74**, 505–518 (1985).
2. Jenkyns, H. C. The early Toarcian (Jurassic) anoxic event: stratigraphic, sedimentary, and geochemical evidence. *Am. J. Sci.* **288**, 101–151 (1988).
3. Hesselbo, S. P. *et al.* Massive dissociation of gas hydrate during a Jurassic oceanic anoxic event. *Nature* **406**, 392–395 (2000).
4. Sælen, G., Tyson, R.V., Telnæs, N. & Talbot, M.R. Constracting watermass conditions during deposition of the Whitby Mudstone (Lower Jurassic) and Kimmeridge Clay (Upper Jurassic) formations, UK. *Palaeogeogr. Palaeoclimatol. Palaeoecol.* **163**, 163–196 (2000).
5. Jenkyns, H. C., Jones, C. E., Grocke, D. R., Hesselbo, S. P. & Parkinson, D. N. Chemostratigraphy of the Jurassic System: applications, limitations and implications for palaeoceanography. *J. Geol. Soc. London* **159**, 351–378 (2002).
6. Kemp, D. B., Coe, A. L., Cohen, A. S. & Schwark, L. Astronomical pacing of methane release in the Early Jurassic period. *Nature* **437**, 396–399 (2005).
7. Hesselbo, S. P., Jenkyns, H. C., Duarte, L. V. & Oliveira, L. C. V. Carbon-isotope record of the Early Jurassic (Toarcian) Oceanic Anoxic Event from fossil wood and marine carbonate (Lusitanian Basin, Portugal). *Earth Planet. Sci. Lett.* **253**, 455–470 (2007).

8. Hermoso, M., Le Callonnec, L., Minoletti, F., Renard, M. & Hesselbo, S. P. Expression of the Early Toarcian negative carbon-isotope excursion in separated carbonate microfractions (Jurassic, Paris Basin). *Earth Planet. Sci. Lett.* **277**, 194–203 (2009).
9. French, K.L., Sepúlveda, J., Trabucho-Alexandre, J., Gröcke, D.R. & Summons, R.E. Organic geochemistry of the early Toarcian oceanic anoxic event in Hawsker Bottoms, Yorkshire, England. *Earth Planet. Sci. Lett.* **390**, 116–127 (2014).
10. Suan, G., van de Schootbrugge, B., Adatte, T., Fiebig, J. & Oschmann, W. Calibrating the magnitude of the Toarcian carbon cycle perturbation. *Paleoceanography* **30**, 495–509 (2015).
11. Duncan, R. A., Hooper, P. R., Rehacek, J., Marsh, J. S. & Duncan, A. R. The timing and duration of the Karoo igneous event, southern Gondwana. *J. Geophys. Res.-Sol. Ea.* **102**, 18127–18138 (1997).
12. McElwain, J. C., Wade-Murphy, J. & Hesselbo, S. P. Changes in carbon dioxide during an oceanic anoxic event linked to intrusion into Gondwana coals. *Nature* **435**, 479–482 (2005).
13. Svensen, H. *et al.* Hydrothermal venting of greenhouse gases triggering Early Jurassic global warming. *Earth Planet. Sci. Lett.* **256**, 554–566 (2007).
14. Dera, G. *et al.* Climatic ups and downs in a disturbed Jurassic world. *Geology* **39** 215–218 (2011).
15. Ullmann, C. V., Thibault, N., Ruhl, M., Hesselbo, S. P. & Korte, C. Effect of a Jurassic oceanic anoxic event on belemnite ecology and evolution. *Proc. Natl. Acad. Sci. USA* **111**, 10073–10076 (2014).
16. Brazier, J. M. *et al.* Calcium isotope evidence for dramatic increase of continental weathering during the Toarcian oceanic anoxic event (Early Jurassic). *Earth Planet. Sci. Lett.* **411**, 164–176 (2015).
17. Jenkyns, H. C. Geochemistry of oceanic anoxic events. *Geochem. Geophy. Geosy.* **11**, Q03004, doi: 10.1029/2009gc002788 (2010).
18. Jenkyns, H. C. Evidence for rapid climate change in the Mesozoic-Palaeogene greenhouse world. *Philos. T. R. Soc. A* **361**, 1885–1916 (2003).
19. Huang, K. *et al*. Sedimentary environments and palaeoclimate of the Triassic and Jurassic in Kuqa River area, Xinjinag (in Chinese with English abstract). *Journal of Palaeogeography* **5**, 197–208 (2003).
20. Yang, Y., Li, W. & Ma, L. Tectonic and stratigraphic controls of hydrocarbon systems in the Ordos basin: A multicycle cratonic basin in central China. *AAPG Bulletin* **89**, 255–269 (2005).
21. He, F. & Zhu, T. Favorable targets of breakthrough and built-up of shale gas in continental facies in Lower Jurassic, Sichuan Basin (in Chinese with English abstract). *Petroleum Geology & Experiment* **34**, 246–251 (2012).
22. Cai, C., Worden, R. H., Bottrell, S. H., Wang, L. & Yang, C. Thermochemical sulphate reduction and the generation of hydrogen sulphide and thiols (mercaptans) in Triassic carbonate reservoirs from the Sichuan Basin, China. *Chem. Geol.* **202**, 39–57 (2003).
23. Guo, T., Li, Y. & Wei, Z. Reservoir-forming conditions of shale gas in Ziliujing Formation of Yuanba Area in Sichuan Basin (in Chinese with English abstract). *Natural Gas Geoscience* **22**, 1–7 (2011).
24. Wang, Y. *et al*. *The terrestrial Triassic and Jurassic Systems in the Sichuan Basin, China*. (University of Science & Technology of China Press, 2010).
25. Wei, M. in *Continental Mesozoic stratigraphy and paleontology in the Sichuan Basin* (in Chinese) 346–363 (People's Publishing House of Sichuan, 1982).
26. Ogg, J. G. & Hinnov, L.A. in *The Geologic Time Scale 2012* Vol. 2 (eds Gradstein, F.M.; Ogg, J.G.; Schmitz, M.D. & Ogg, G.M.) Ch. 26, 731–791 (Elsevier, 2012).
27. Hallam, A. A revised sea-level curve for the Early Jurassic. *J. Geol. Soc. London* **138**, 735–743 (1981).

28. Suan, G. *et al.* Polar record of Early Jurassic massive carbon injection. *Earth Planet. Sci. Lett.* **312**, 102–113 (2011).
29. Percival, L.M.E., Cohen, A.S., Davies, M.K., Dickson, A.J., Hesselbo, S.P., Jenkyns, H.C., Leng, M.J., Mather, T.A., Storm, M.S. & Xu, W. Osmium isotope evidence for two pulses of increased continental weathering linked to Early Jurassic volcanism and climate change. *Geology* doi: 10.1130/G37997.1 (2016).
30. Moldowan, J. M., Seifert, W. K. & Gallegos, E. J. Relationship between petroleum composition and depositional environment of petroleum source rocks. *AAPG Bulletin* **69**, 1255–1268 (1985).
31. Holba, A. G., Tegelaar, E., Ellis, L., Singletary, M. S. & Albrecht, P. Tetracyclic polyprenoids: Indicators of freshwater (lacustrine) algal input. *Geology* **28**, 251–254 (2000).
32. Vakhrameyev, V. A. Pollen *Classopollis*: indicator of Jurassic and Cretaceous climate. *Paleobotanist* **28-29**, 301–307 (1981).
33. Kürschner, W. M., Batenburg, S. J. & Mander, L. Aberrant *Classopollis* pollen reveals evidence for unreduced (2n) pollen in the conifer family Cheirolepidiaceae during the Triassic–Jurassic transition. *Proc. Biol. Sci.* **280**, 20131708 (2013).
34. Boos, W.R. & Kuang, Z. Dominant control of the South Asian monsoon by orographic insulation versus plateau heating. *Nature* **463**, 218–222 (2010).
35. Wilkin, R. T. & Barnes, H. L. Pyrite formation by reactions of iron monosulfides with dissolved inorganic and organic sulfur species. *Geochim. Cosmochim. Acta* **60**, 4167–4179 (1996).
36. Dahl, T. W. *et al.* Tracing euxinia by molybdenum concentrations in sediments using handheld X-ray fluorescence spectroscopy (HHXRF). *Chem. Geol.* **360**, 241–251 (2013).
37. Sinninghe Damsté, J. S. *et al.* Evidence for Gammacerane as an indicator of water column stratification. *Geochim. Cosmochim. Acta* **59**, 1895–1900 (1995).
38. Kemp, D. B., Coe, A. L., Cohen, A. S. & Weedon, G. P. Astronomical forcing and chronology of the early Toarcian (Early Jurassic) oceanic anoxic event in Yorkshire, UK. *Paleoceanography* **26**, PA4210, doi:10.1029/2011pa002122 (2011).
39. Suan, G. *et al.* Duration of the Early Toarcian carbon isotope excursion deduced from spectral analysis: Consequence for its possible causes. *Earth Planet. Sci. Lett.* **267**, 666–679 (2008).
40. Boulila, S. *et al.* Astronomical calibration of the Toarcian Stage: Implications for sequence stratigraphy and duration of the early Toarcian OAE. *Earth Planet. Sci. Lett.* **386**, 98–111 (2014).
41. Beerling, D. J. & Brentnall, S.J. Numerical evaluation of mechanisms driving Early Jurassic changes in global carbon cycling. *Geology* **35**, 247–250 (2007).
42. Zou, C. in *Unconventional Petroleum Geology*. Ch. 3, 61–109 (Petroleum Industry Press, 2013).
43. Dean, W.E. & Gorham, E. Magnitude and significance of carbon burial in lakes, reservoirs, and peatlands. *Geology* **26**, 535–538 (1998).
44. Cohen, A. S., Coe, A. L., Harding, S. M. & Schwark, L. Osmium isotope evidence for the regulation of atmospheric CO_2 by continental weathering. *Geology* **32**, 157–160 (2004).

Acknowledgements Shell International Exploration & Production B.V. is acknowledged for financial support for this study. D.S. acknowledges the Total endowment fund. R.D.P. and B.D.A.N. acknowledge funding from the advanced ERC

grant “the greenhouse earth system” (T-GRES, project reference 340923). All authors thank Shell Global Solutions International B.V., Shell China Exploration & Production Co. Ltd, and PetroChina Southwest Oil and Gasfield Company for approval to publish this study. J.B.R. publishes with the approval of the Executive Director, British Geological Survey (NERC). CGG Robertson and Shell are acknowledged for providing the palaeogeographic reconstruction used in Figure 1. Tai-Ran Jiang, Malcolm Dransfield and Xue-Yan Li (Shell China Exploration and Production Co. Ltd.), Olaf Podlaha, Sander van den Boorn (Shell Global Solutions International B.V.), Qinggao Zeng and Zhiping Tang (PetroChina Southwest Oil and Gasfield Company) and Bruce Levell (University of Oxford) are acknowledged for discussions and reviews of earlier versions of the manuscript and for providing sample materials. We also thank reviewers David Kemp and Guillaume Suan and an anonymous reviewer for comments and suggestions that have greatly improved this manuscript. This paper is also a contribution to UNESCO-IUGS IGCP Project 632.

Author contribution statement

W. X., M.R., H.C.J. and S.P.H. designed the project. W.X. and M.R. performed core description and sampling. W.X., M.R., J.B.R., D.S., J.W.H.W. and B.D.A.N. performed geochemical and palynological analyses. All authors contributed to data analysis and interpretation and writing and/or refinement of the manuscript.

Additional information

Supplementary information is available in the online version of the paper. Reprints and permissions information is available online at www.nature.com/reprints. Correspondence and requests for materials should be addressed to W. X.

442

443 **Competing financial interests**

444 The authors declare no competing financial interests.

445

446 **Figure captions**

447 **Figure 1 Size and location of the palaeo-Sichuan lake at 179 Ma.** The map on
448 the left shows a regional tectonic plate reconstruction at 179 Ma (edited from a map
449 provided by CGG Robertson and Shell), with positions of the latest Early Jurassic
450 lacustrine Sichuan, Tarim and Ordos Basins marked[21,23,42]. The map on the right
451 illustrates the location of the two cores studied within the Sichuan Basin; relative
452 variations in lake depth are illustrated in blue, with the darker shade representing
453 deeper water areas; the green brickwork represents fossiliferous limestone and the
454 yellow dotted ornaments represent deltaic deposits; palaeo-mountain ranges are
455 marked in brown and thickness of the Da'anzhai Member is indicated by the isopachs.

456 **Figure 2 Stratigraphic correlation of cores A and B and**
457 **palaeoenvironmental proxies in the Sichuan Basin (China).** Stratigraphic changes
458 in lithology from each core are illustrated by Ca concentrations (from XRF
459 measurements on the core-slabs) superimposed on the combined core photos, with
460 light colours representing limestone and dark colours representing shale. $\delta^{13}C_{TOC}$
461 from both cores are plotted in red squares and the 3-point moving averages are plotted
462 in thick red lines. $\delta^{13}C_{n\text{-alkane}}$ data from different chain-lengths are plotted in diamonds
463 of different colours, as illustrated in the legend. Error bars on $\delta^{13}C_{n\text{-alkane}}$ data reflect
464 the 1σ standard deviation of replicates. TOC and HI values from Rock-Eval pyrolysis
465 are plotted for both cores in black and dark blue squares, respectively (note similar
466 pattern of TOC enrichment). The Gammacerane Index values (Gammacerane/C_{30}

Hopane) are plotted in yellow diamonds. Marine acritarch percentages (%) are plotted in the larger blue squares with light blue shades. Ratios of *Classopollis sp.* tetrads *vs* single grains are plotted in black squares.

Figure 3 Geochemical comparison between the lacustrine Da'anzhai Member (Sichuan Basin, China) and the lower Toarcian marine succession from Yorkshire (UK). Re-Os (Rhenium-Osmium) isochrons from both Yorkshire[44] and the Da'anzhai Member (Sichuan Basin; this study) are plotted with short dashed lines, indicating the depths of samples that produced the Re-Os isochrons. The Re-Os isochron from the upper Lower Jurassic lacustrine Da'anzhai Member (Core A) gives an age of 180.3±3.2 Ma, and the Lower Toarcian marine Jet Rock (Yorkshire) gives a Re-Os isochron age of 178.2±5.6 Ma[44]. The two successions are correlated based on $\delta^{13}C_{TOC}$ and $\delta^{13}C_{n\text{-alkane}}$ from the Da'anzhai Member, and $\delta^{13}C_{TOC}$[6,44], $\delta^{13}C_{n\text{-alkane}}$[9] and $\delta^{13}C_{phytane}$[4] from Yorkshire. S and Mo concentrations (from XRF measurements) and TOC (from Rock Eval pyrolysis) on Core A are plotted in yellow lines, blue diamonds and black lines with dark grey shades, respectively. TOC and S records from Yorkshire[38] are plotted in yellow lines and black lines with dark grey shades, respectively. A conservatively estimated ~460 Gt organic carbon was buried in the palaeo-Sichuan lake system during the T-OAE.

Figure 4 Model for the formation of lacustrine conditions in the Sichuan Basin. On the right are idealized $\delta^{13}C$ records across the T-OAE, with the stratigraphic intervals marked with grey shading representing the different phases in lake evolution. Phase A: the continental Sichuan Basin was marked by fluvial and terrestrial sedimentary deposition pre-T-OAE negative CIE, with possibly geographically restricted lacustrine conditions in the central part of the basin. Phase B: early Toarcian temperature and sea-level rise increased evaporation from the

approaching marine waters, enhancing the hydrological cycle and promoting precipitation in the continental interior of the Sichuan Basin, which resulted in the formation or strong expansion of the palaeo-Sichuan lake. Phase C: continuing late Early Toarcian eustatic sea-level rise allowed for occasional marine incursions into the dominantly lacustrine palaeo-Sichuan basin. Phase D: eustatic sea-level fall in the latest Early Toarcian initiated the return to fully lacustrine conditions and maximum marine and lacustrine organic carbon burial. Phase E: global recovery from the Early Toarcian climatic perturbation, with associated reduction in global temperature and cessation of enhanced hydrological cycling, initiated the return to a terrestrial and fluvial depositional environment in the Sichuan Basin.

METHODOLOGY

[1] GEOLOGICAL SETTING OF THE SICHUAN BASIN

The Sichuan Basin formed on the western part of the Yangtze Platform, in which sedimentation commenced with the Neoproterozoic Sinian Sequence (850–570 Ma)[45]. Shallow-marine carbonates formed from the Tonian to the Middle Triassic, with occasional epeirogenic events, e.g. widespread basalt emplacement due to extension of the western margin of the Yangtze Platform, in the Late Palaeozoic[45]. Sedimentation switched from marine to continental in the Middle to Late Triassic with Indosinian tectonic uplift due to closure of the Palaeotethys and collision of the North and South China cratonic blocks[22]. Siliciclastic sediments were deposited as alluvial fans and lakeshore–deltaic plain facies in the Early Jurassic, particularly along the southern front of the Longmen and Micang-Daba mountain ranges at the northwestern and northern margins of the Sichuan Basin[21,23,42,45] (Fig. 1).

517 Continental/fluvial deposits and green/red pedogenic horizons with soil carbonate
518 nodules mark the Ma'anshan Member (middle Ziliujing Formation) and underlie the
519 lacustrine facies of the upper Lower Jurassic Da'anzhai Member (uppermost Ziliujing
520 Formation). The Da'anzhai Member represents the development of dominantly
521 lacustrine conditions and the formation of a major lake. Lacustrine conditions may,
522 however, have persisted through most of the Early Jurassic in the most central and
523 deepest part of the basin, although their onset and termination are still poorly dated[46].
524
525 [2] AGE MODEL
526 Re-Os radiometric dating on 16 samples from two combined intervals of the
527 Da'anzhai lacustrine black shale (Core A) shows a well-constrained single isochron of
528 180.3±3.2 Ma (Fig. 3; Supplementary Information Fig. S1), constraining the
529 Da'anzhai Member to the Toarcian, following the Jurassic timescale of Ogg and
530 Hinnov (2012)[26]. A Re-Os isochron for the organic-rich marine mudrock from the
531 *falciferum* ammonite subzone in Yorkshire (UK) suggests a depositional age of
532 178.2±5.6 Ma[44]. The age obtained here for the lacustrine Da'anzhai Member in the
533 Sichuan Basin is in agreement, within uncertainty, with the marine realm early
534 Toarcian Re-Os isochron-based age (Fig. 3; Supplementary Information Fig. S2).
535 The palynomorph assamblages of the lacustrine Da'anzhai Member, with the
536 superabundance of the pollen *Classopollis* sp. (and the absence of *Callialasporites*
537 spp.), the occurrence of the spore *Ischyosporites vaerigatus*, the acritarch
538 *Veryhachium collectum*, multi-specimen clumps of the prasinophyte *Halosphaeropsis*
539 *liassica* and the rare occurrence of the dinoflagellate cyst ?*Skuadinium* sp., are
540 comparable to floras from lower Toarcian marine successions in northern Europe and
541 Australia, indicating that the successions studied here are of similar age

542 (Supplementary Information Fig. S4 shows a range chart with selected palynomorph
543 occurrence). The superabundance of the thermophylic pollen genus *Classopollis* and
544 the occurrence of the opportunistic prasinophyte species *Halosphaeropsis liassica,*
545 thought to have thrived in environmentally stressed conditions and normally
546 occurring in multi-specimen clumps, are especially typical of the T-OAE
547 (Supplementary Information)[47–50].

548 Furthermore, $\delta^{13}C_{TOC}$ analyses of Core A reveal <3‰ fluctuations in the basal
549 15 m of the Da'anzhai Member, followed by a transient ~4‰ negative excursion (Fig.
550 2). The base of Core B is interpreted to be stratigraphically younger than Core A
551 based on carbon-isotope correlation, and similarly shows a ~4‰ negative excursion
552 in $\delta^{13}C_{TOC}$ (Fig. 2), followed by a full positive return to initial base values. The two
553 cores combined illustrate the complete negative CIE, which is similar in shape and
554 magnitude to that observed in marine records of the T-OAE (Fig. 3)[6,44]. Compound-
555 specific long-chain *n*-alkane (C_{23}–C_{33}) $\delta^{13}C$ analyses of Core A also show a distinct
556 ~4‰ negative excursion, similar in magnitude to the bulk organic-matter $\delta^{13}C_{TOC}$
557 from the same stratigraphic interval (Figs 2 and 3). Long-chain *n*-alkanes in
558 sedimentary organic matter are typically sourced from terrestrial higher plants or
559 freshwater algae[51] whose isotopic compositions are commonly indistinguishable
560 because lake-water dissolved inorganic carbon (DIC) is isotopically in equilibrium
561 with the atmosphere[52]. Consequently, the observed shift in $\delta^{13}C_{n\text{-alkanes}}$ directly reflects
562 changes in the carbon-isotope composition of the atmosphere (and lake-water DIC)
563 during the early Toarcian global carbon-cycle perturbation. The odd-over-even
564 predominance in the long-chain (C_{23}−C_{33}) *n*-alkane distribution, typical for terrestrial
565 higher plant leaf waxes or freshwater algal-sourced sedimentary organic matter[51] is,
566 however, not observed from Core A (with a Carbon Preference Index of ~1), probably

567 due to its relatively elevated thermal maturity[53]. The ~2–3‰ carbon-isotope
568 fluctuations in $\delta^{13}C_{TOC}$ in the lower Da'anzhai Member of Core A (2702–2715m in
569 the core) are, however, not repeated in the $\delta^{13}C_{n\text{-alkane}}$ record. This feature may suggest
570 a shift in the dominant sedimentary organic matter source away from freshwater algae
571 to ^{13}C-enriched terrestrial woody organic matter, with HI values of <100 mg HC/g
572 TOC at 2711.4–2712.3m and 2703.5–2706.6m in the lower Da'anzhai Member of
573 Core A, which are much lower than HI values of the upper Da'anzhai Member, where
574 the degree of maturity is similar (Fig. 2; see Supplementary Information for further
575 discussion).

576 Overall, relatively enriched $\delta^{13}C_{TOC}$ values in the more proximal Core B may
577 be explained by the greater woody component of terrestrial residual sedimentary
578 organic matter (the isotopically heavier ligno-cellulose component of a plant)[3,54], as
579 suggested indirectly by low HI values (<200 mg HC/g TOC; Fig. 2) and directly by
580 palynological study (with 26–45% wood). In addition, the more proximal Core B is
581 thermally more mature, with Tmax values mainly of 453–470°C (Tmax values of
582 Core A are mainly 444–460°C). Maturation of kerogen can increase its $\delta^{13}C_{TOC}$
583 values by 1–2‰, which may have further contributed to the offset observed between
584 the organic-carbon isotope records of cores A and B[55]. The observed parallel
585 signature in $\delta^{13}C_{TOC}$ and $\delta^{13}C_{n\text{-alkane}}$ in the main phase of the Da'anzhai Member
586 (above 2698 m) therefore likely reflects a true perturbation of the global exogenic
587 carbon cycle. It is similar in shape and magnitude to what is characteristically
588 observed in lower Toarcian marine calcite and compound-specific marine and
589 terrestrial organic matter from Europe and elsewhere spanning the T-OAE[4,8–10] (Fig.
590 3).
591

[3] TERRESTRIAL ENVIRONMENT

The consistent superabundance in both cores of the thermophylic pollen genus *Classopollis*, which is thought to have derived from gymnosperm conifers dwelling in regions marginal to bodies of water[32], suggests higher temperature conditions in the continental interior or along the shorelines of the palaeo-Sichuan lake system. Elevated atmospheric and marine temperatures during the T-OAE have also been suggested from coeval marine records, also with increased abundance of *Classopollis* and the ^{18}O-depleted signature of macrofossil calcite[14,18,32].

Data availability

The authors declare that the data supporting the findings of this study are available within the article and its supplementary information files.

45. Ryder, R. T. *Petroleum Geology of the Sichuan Basin, China: Report on U.S. Geological Survey and Chinese Ministry of Geology and Mineral Resources Field Investigations and Meetings, October 1991*. (U.S. Geological Survey, 1994).
46. Li, Y. & He, D. Evolution of tectonic-depositional environment and prototype basins of the Early Jurassic in Sichuan Basin and adjacent areas (in Chinese with English abstract). *Acta Petrolei Sinica* **35**, 219–232 (2014).
47. Wall, D. Microplankton, pollen, and spores from the Lower Jurassic in Britain. *Micropaleontology* **11**, 151–190 (1965).
48. Dybkjær, K. Palynological zonation and palynofacies investigation of the Fjerritslev Formation (Lower Jurassic-basal Middle Jurassic) in the Danish Subbasin. *Danmarks Geologiske Undersøgelse Serie A*, Nr. **30**, 150 p. (1991).
49. Bucefalo Palliani, R., Mattioli, E. & Riding, J. B. The response of marine phytoplankton and sedimentary organic matter to the early Toarcian (Lower Jurassic) oceanic anoxic event in northern England. *Mar. Micropaleontol.* **46**, 223–245 (2002).
50. Riding, J. B. & Helby, R. Early Jurassic (Toarcian) dinoflagellate cysts from the Timor Sea, Australia. *Memoir of the Association of Australasian Palaeontologists* **24**, 1–32 (2001).
51. Lichtfouse, E., Derenne, S., Mariotti, A. & Largeau, C. Possible Algal origin of long-chain odd *n*-alkanes in immature sediments as revealed by distributions and carbon-isotope ratios. *Org. Geochem.* **22**, 1023–1027 (1994).
52. Meyers, P. Preservation of elemental and isotopic source identification of sedimentary organic matter. *Chem. Geol.* **114**, 289–302 (1994).
53. Meyers, P. & Ishiwatari, R. in *Org. Geochem.* Vol. 11 *Topics in Geobiology* (eds. Engel, M. H. & Macko, S.A.) Ch. 8, 185–209 (Springer US, 1993).
54. van Bergen, P.F. & Poole, I. Stable carbon isotopes of wood: a clue to palaeoclimate? *Palaeogeogr. Palaeoclimatol. Palaeoecol.* **182**, 31–45 (2002).

631 55. Whelan, J. & Thompson-Rizer, C. in *Org Geochem* Vol. 11 *Topics in Geobiology*
632 (eds. Engel, M.H. & Macko, S.A.) Ch. 14, 289–353 (Springer US, 1993).

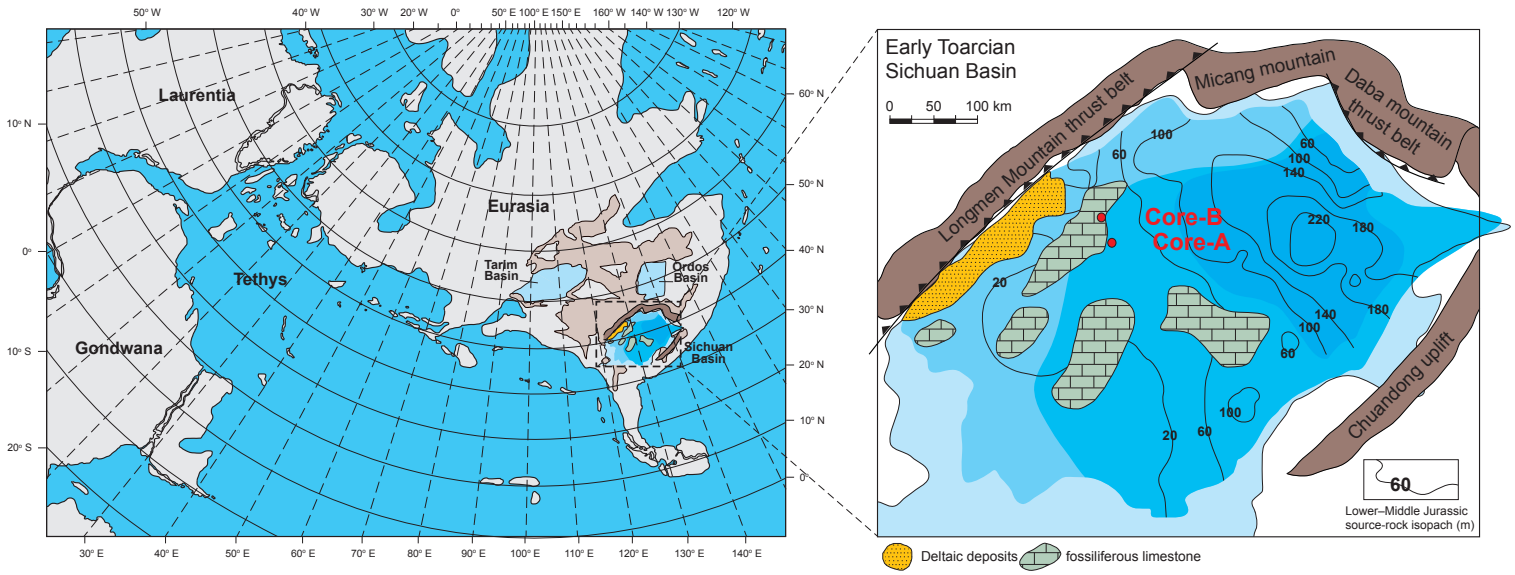
Laurentia
Eurasia
Tethys
Gondwana
Tarim Basin
Ordos Basin
Sichuan Basin
Early Toarcian
Sichuan Basin
0 50 100 km
Longmen Mountain thrust belt
Micang mountain
Daba mountain thrust belt
Chuandong uplift
Core-B
Core-A
60
Lower–Middle Jurassic source-rock isopach (m)
Deltaic deposits
fossiliferous limestone

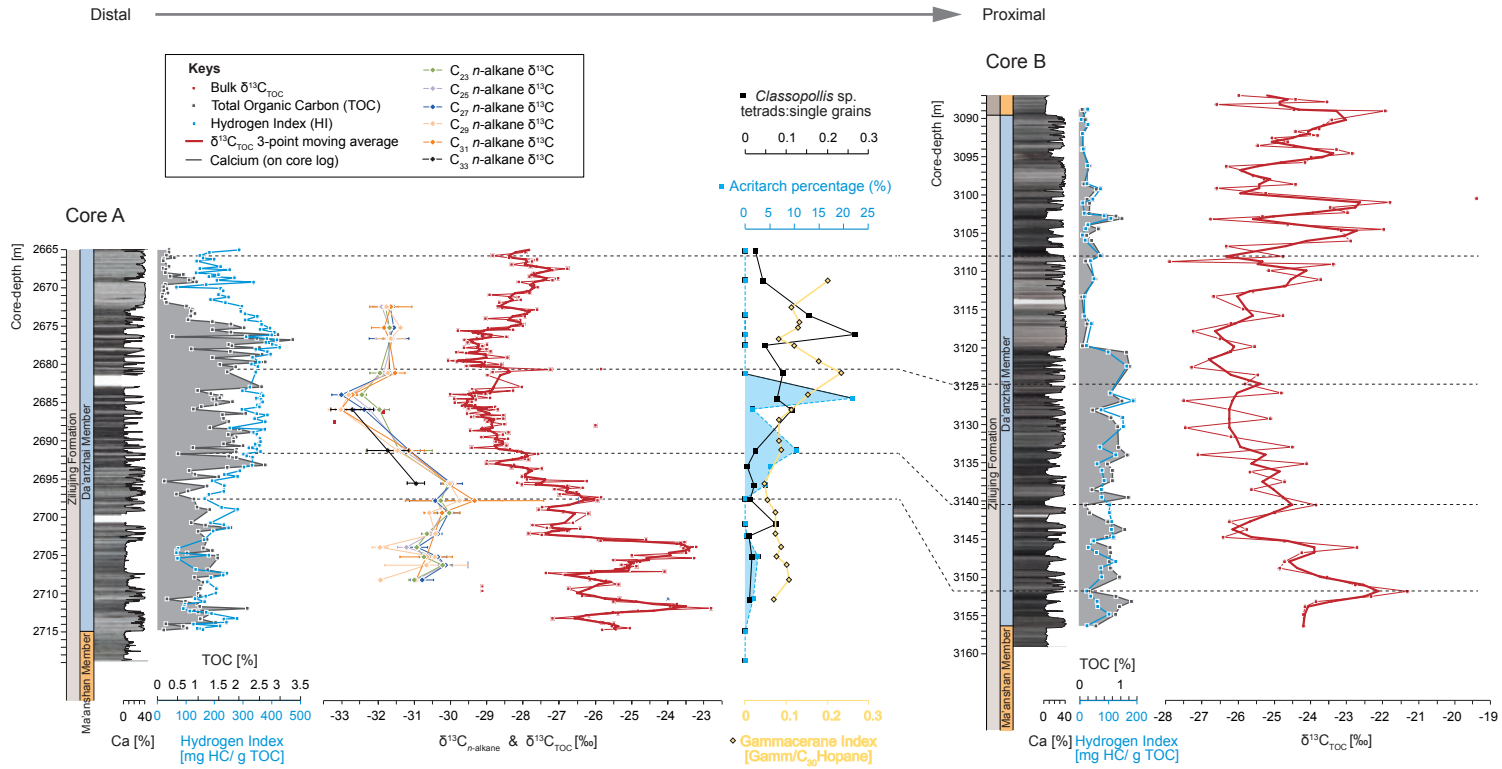
Distal
Proximal
Keys
Bulk δ13CTOC
Total Organic Carbon (TOC)
Hydrogen Index (HI)
δ13CTOC 3-point moving average
Calcium (on core log)
C23 n-alkane δ13C
C25 n-alkane δ13C
C27 n-alkane δ13C
C29 n-alkane δ13C
C31 n-alkane δ13C
C33 n-alkane δ13C
Classopollis sp. tetrads:single grains
Acritarch percentage (%)
Core A
Core B
Core-depth [m]
Zhuqing Formation
Da'anzhai Member
Ma'anshan Member
TOC [%]
Ca [%]
Hydrogen Index [mg HC/ g TOC]
δ13Cn-alkane & δ13CTOC [‰]
Gammacerane Index [Gamm/C30Hopane]
δ13CTOC [‰]

MARINE REALM

Lower Toarcian Marine Black Shales [Yorkshire, UK]

LACUSTRINE REALM

Lower Toarcian Lacustrine Black Shales [Sichuan Basin, China]

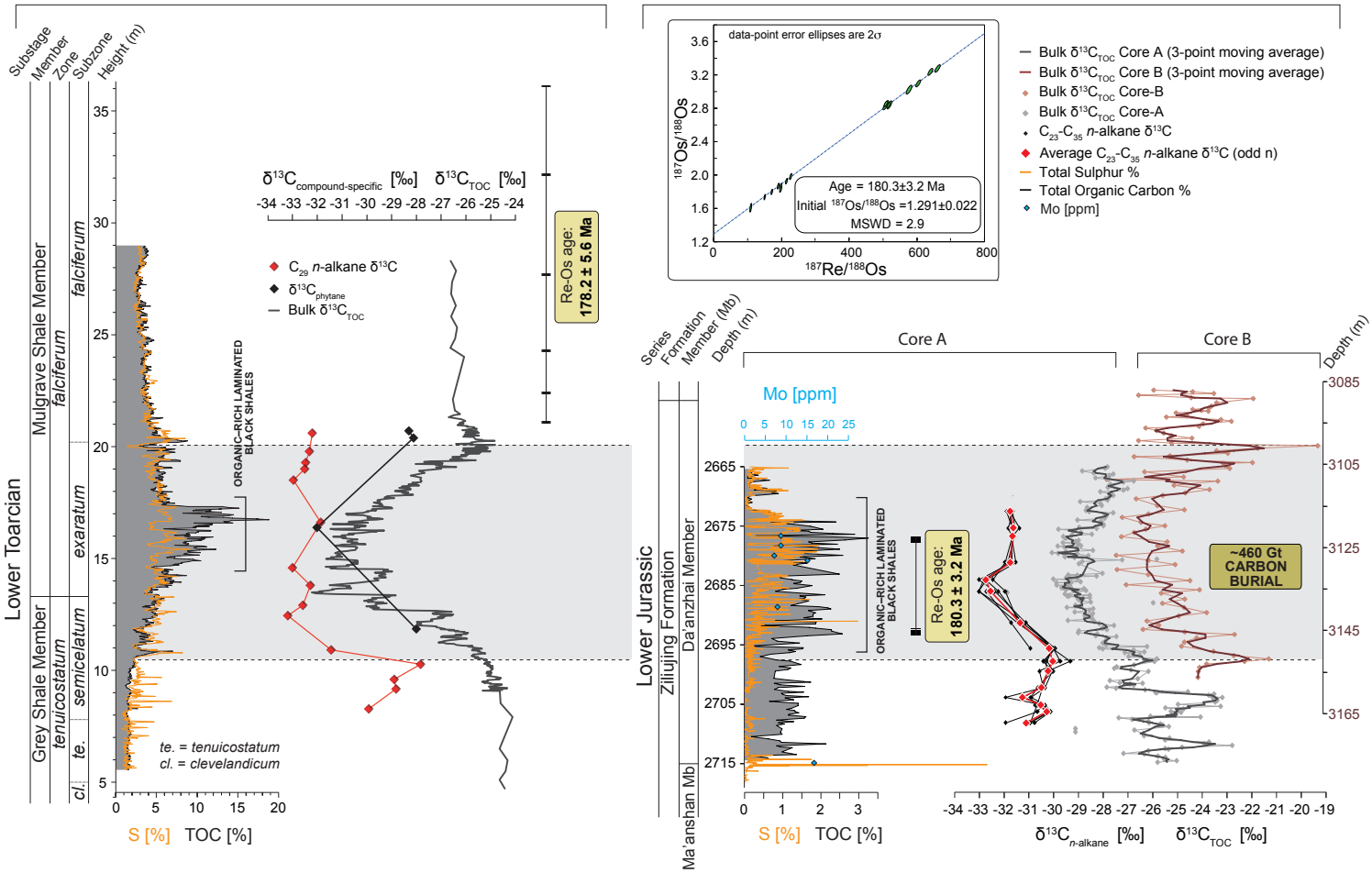

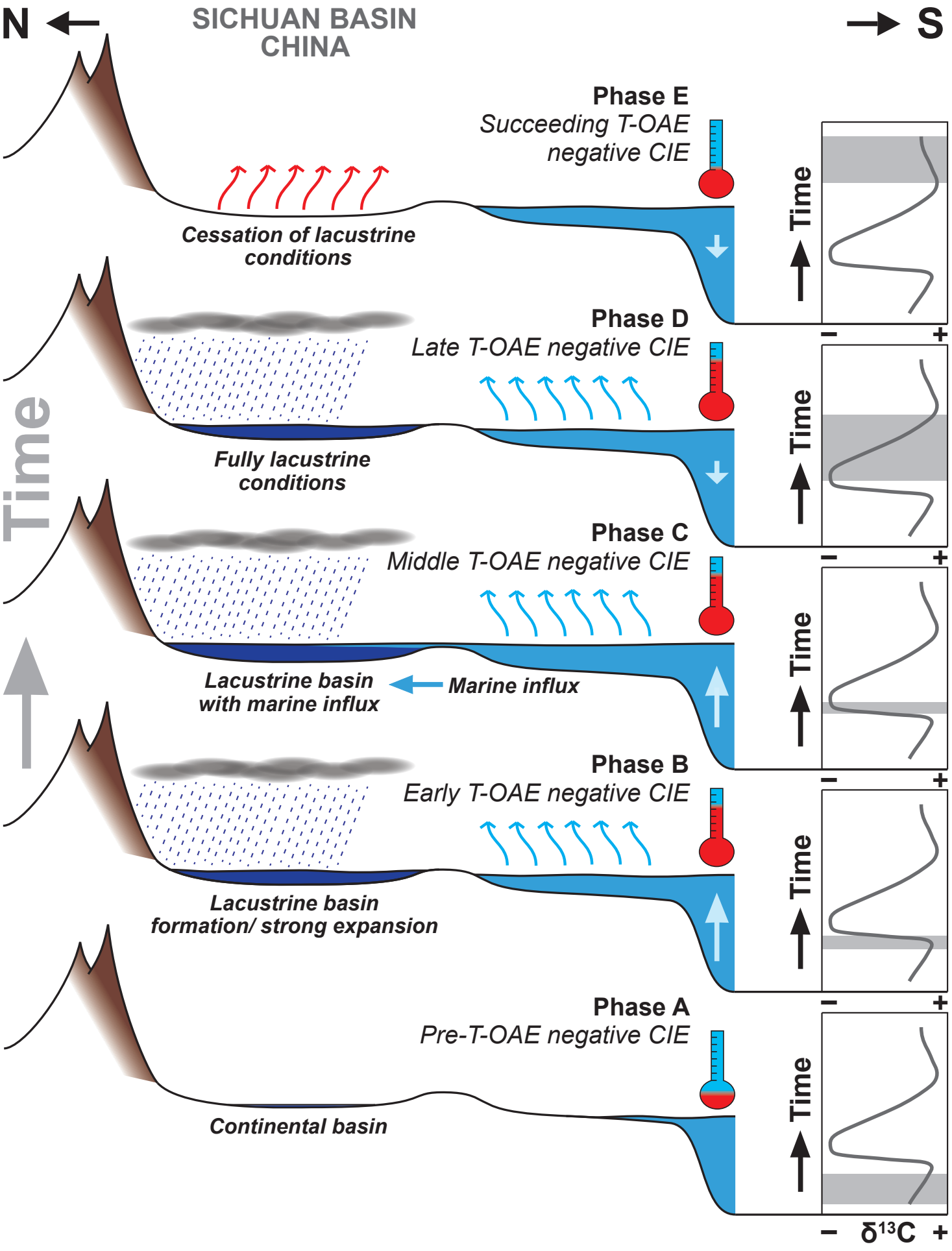
N
SICHUAN BASIN
CHINA
S
Phase E
Succeeding T-OAE
negative CIE
Cessation of lacustrine
conditions
Phase D
Late T-OAE negative CIE
Fully lacustrine
conditions
Phase C
Middle T-OAE negative CIE
Lacustrine basin
with marine influx
Marine influx
Phase B
Early T-OAE negative CIE
Lacustrine basin
formation/ strong expansion
Phase A
Pre-T-OAE negative CIE
Continental basin
Time
Time
Time
Time
Time
Time
Time
– +
– +
– +
– +
– δ13C +